This article has been accepted for publication in a future issue of this journal, but has not been fully edited. Content may change prior to final publication. Citation information: DOI 10.1109/JSEN.2015.2413057, IEEE Sensors Journal

Colorimetric analysis for on-line arc-welding diagnostics by means of plasma optical spectroscopy

Jesus Mirapeix Serrano, Ruben Ruiz Lombera, Jose J. Valdiande, Adolfo Cobo (*Member, IEEE*) and Jose Miguel Lopez-Higuera (*Senior Member, IEEE*)

***Abstract*— In this paper an analysis on the suitability of employing a colorimetric analysis of the acquired plasma spectra to perform online arc-welding quality monitoring will be discussed. Different colorimetric parameters like the color temperature or the parameters associated with the HSL color space will be evaluated in comparison to the standard approach based on the estimation of the plasma electronic temperature. This approach does not require the identification of the emission lines involved in the analysis, thus giving rise to a more efficient solution in terms of computational efficiency, and avoiding unambiguous identifications that may give rise to incorrect results. In particular, experimental tests performed with a TIG (Tungsten Inert Gas) arc-welding process will show the feasibility of using the proposed solution and its ability to perform an online detection of different welding perturbations.**

***Index Terms*— optical fiber sensor; on-line monitoring; plasma spectroscopy; arc-welding; quality assurance; colorimetry**

I. Introduction

DIFFERENT industrial scenarios involve an extensive employment of welding processes, like the manufacturing of automobiles, aeronautics or the naval or energy sectors, just to mention some examples. In some of these situations the requirements in terms of the associated quality standards are very demanding, thus giving rise to the necessity of assessing the final quality of those products. Although nowadays different NDT (Non-destructive techniques) are employed to detect possible defects once the seam has been created, an intense research effort has been devoted in the last years to find reliable monitoring solutions able to provide information in real time about these processes.

In this regard there are a wide range of different approaches that go from machine vision [1], even with sophisticated setups to obtain an optimal vision of the weld pool by means of laser illumination [2], to infrared thermography [3], or electrical [4] or acoustic monitoring [5]. The analysis of the light emitted by the plasma formed during the welding process by means of plasma optical spectroscopy is a very promising solution in this regard. It is worth noting that this approach allows to access the information associated with the atomic emission lines of the different species involved in the process, thus enabling a powerful analysis. The so-called traditional spectroscopic approach is based on the estimation of the plasma electronic temperature T_e, given the known correlation between this parameter and the quality of the associated seams [6]. The method to obtain T_e commonly only relies in the use of a single plasma species and the sensitivity of this parameter to different welding flaws may vary, thus compromising the system performance [6]. In addition, the calculation of T_e requires several processing stages [7], where the line identification step might be complicated. On the one hand, this stage might be the most demanding in terms of computational times if a real-time identification is needed. On the other hand, and most importantly, an unambiguous identification of the emission lines might prove especially difficult depending on the optical resolution of the spectrometers involved and the elements participating in the process.

In this regard, the employment of monitoring approaches avoiding this requirement would be interesting, like the analysis of the plasma continuum radiation [8], the line-to-continuum method [9] or the use of the plasma-RMS signal [10]. Within this framework, we propose the use of a colorimetric approach to carry out the welding diagnostics. Although a few works have dealt with solutions based on colorimetry [11], none of them has offered a detailed comparison between the results derived from both T_e and the colorimetric parameters for different welding perturbations. In this paper we propose the employment of a colorimetric approach for welding monitoring based on the use of the HSL color space and the color temperature. The feasibility of this

This paper has been submitted for review on January 16, 2015.
This work has been supported by the project TEC2013-47264-C2-1-R.
J. Mirapeix is with the University of Cantabria, Santander, 39005 Spain (e-mail: jesus.mirapeix@unican.es).
R. Ruiz-Lombera is with the University of Cantabria, Santander, 39005 Spain (e-mail: ruben.ruiz@unican.es).
J. Valdiande is with the University of Cantabria, Santander, 39005 Spain (e-mail: jose.valdiande@unican.es).
A. Cobo is with the University of Cantabria, Santander, 39005 Spain (e-mail: Adolfo.cobo@unican.es).
J.M. Lopez-Higuera is with the University of Cantabria, Santander, 39005 Spain (e-mail: miguel.lopezhiguera@unican.es).
An earlier version of this paper was presented (oral presentation) at the IEEE Sensors 2014 Conference and was published in its Proceedings
http://ieeexplore.ieee.org/xpl/articleDetails.jsp?tp=&arnumber=6985079

This article has been accepted for publication in a future issue of this journal, but has not been fully edited. Content may change prior to final publication. Citation information: DOI 10.1109/JSEN.2015.2413057, IEEE Sensors Journal

solution will be explored by means of arc-welding tests.

II. Plasma Optical Spectroscopy and Colorimetric Approach for Welding Diagnostics

A. Plasma Optical Spectroscopy

When plasma optical spectroscopy is used for welding diagnostics and T_e is chosen as the output parameter, it is typical to employ a simplified expression for its estimation, where only two emission lines for the same species (same element in the same ionization stage) are involved:

$$T_e = \frac{E_m(2)-E_m(1)}{kln\left[\frac{I(1)A(2)g_m(2)\lambda(1)}{I(2)A(1)g_m(1)\lambda(2)}\right]}, \quad (1)$$

where E_m is the upper level energy of state m, k the Boltzmann constant, I the emission line intensity, A the transition probability, g the statistical weight and λ the wavelength for the emission lines *1* and *2*.

A more accurate estimation of the plasma temperature can be obtained via the Boltzmann plot method, which can be derived from the Boltzmann equation and the expression relating the intensity of a given emission line to the population density of the upper level. In this case, several emission lines should be used in the following expression:

$$ln\left(\frac{I_{mn}\lambda_{mn}}{A_{mn}g_m}\right) = ln\left(\frac{hcN}{Z}\right) - \frac{E_m}{kT_e}, \quad (2)$$

where h is the Planck constant, c the light velocity, N the population density (of state m) and Z the partition function. To obtain T_e with this method it is necessary to represent the left hand-side of Eq. (2) versus E_m, and then apply a linear regression to the points in the plot derived from the different lines. The latter typically avoids its use in real-time scenarios, as Eq. (1) is more efficient in terms of the computational times involved and the accuracy in the estimation of T_e is not so relevant for industrial applications. In addition, the use of more emission lines increases the probability of incorrect identifications, thus giving rise to unexpected results.

B. Colorimetric analysis via color temperature and the HSL color space

The vision process in human beings is defined by two different photoreceptors: cones and rods. The former are those responsible for color vision, and are divided into three types: S, M and L cones (for short, medium and long (wavelengths), associated with the detection of wavelengths with peaks at approximately 420 to 440, 534 to 545 and 564 to 580 nm). To perform a colorimetric analysis it is necessary to previously define the curves associated with the spectral sensitivity of these three detectors, i.e. a color space. A color space can be defined as a completely specified scheme for describing the color of light, typically involving three numerical values or coordinates [12], thus matching the three types of cones previously described. Among the different color spaces available, the CIE (International Commission of Illumination) XYZ color space has been widely employed in scientific studies and other color spaces, like RGB or HSL are typically referred to it [13].

TABLE I
Constants for XYZ to RGB Conversion

M			M^{-1}		
0.48872	0.31068	0.20060	2.37067	-0.90004	-0.47063
0.17620	0.81298	0.01081	-0.51388	1.42530	0.08858
0	0.01020	0.98979	0.00530	-0.01469	1.00940

The values of XYZ, also called the *tristimulus* values, can be obtained by using the following expressions:

$$X = \int_\lambda \bar{x}(\lambda)P(\lambda)d\lambda$$
$$Y = \int_\lambda \bar{y}(\lambda)P(\lambda)d\lambda \quad (3)$$
$$Z = \int_\lambda \bar{z}(\lambda)P(\lambda)d\lambda$$

In Eq. (3) $\bar{x}(\lambda)$, $\bar{y}(\lambda)$ and $\bar{z}(\lambda)$ are the numerical response of the chromatic response of a standard observer and $P(\lambda)$ is the spectral power distribution for the color under analysis. The CIE 1931 Standard Observer, defined to represent an average human chromatic response within a 2º arc inside the fovea, has been used in the present study [14]. Once the values of XYZ have been obtained employing the CIE curves, it is possible to derive the values of the coordinates associated with other color spaces, like RGB. This conversion only requires the employment of nine constants that were also established by CIE [15] (see Table I) using Eq. (4).

$$\begin{bmatrix} X \\ Y \\ Z \end{bmatrix} = [M] \begin{bmatrix} R \\ G \\ B \end{bmatrix} \quad (4)$$

Finally, the HSL (Hue, Saturation, Luminance (Luminosity or brightness)) parameters can be obtained from the RGB components. It is worth mentioning that different HSL spaces have been proposed [16], but in this work the following implementation has been used:

$$H = \begin{cases} 0 & \text{if } MAX = MIN \\ \left(60\frac{G-B}{MAX-MIN} + 360\right) mod\ 360 & if\ MAX = R \\ 60\frac{B-R}{MAX-MIN} + 120 & if\ MAX = G \\ 60\frac{R-G}{MAX-MIN} + 240 & if\ MAX = B \end{cases} \quad (4)$$

$$L = \frac{1}{2}(MAX + MIN) \quad (5)$$

$$S = \begin{cases} 0 & \text{if } MAX = MIN \\ \frac{MAX-MIN}{MAX+MIN} = \frac{MAX-MIN}{2L} & if\ L \le 1/2 \\ \frac{MAX-MIN}{2-(MAX-MIN)} = \frac{MAX-MIN}{2-2L} & if\ L \ge 1/2 \end{cases} \quad (6)$$

This article has been accepted for publication in a future issue of this journal, but has not been fully edited. Content may change prior to final publication. Citation information: DOI 10.1109/JSEN.2015.2413057, IEEE Sensors Journal

In the previous equations *MAX = max (R,G,B)* and *MIN = min (R,G,B)*.

Apart from the HSL parameters, the color temperature has also been considered as a suitable monitoring parameter in this work. For a given light source its color temperature can be defined as the temperature associated with a blackbody (*Planckian* radiator) that emits radiation of the same chromaticity [17]. Its estimation has been performed in this paper using the Robertson's method [17], where two chromaticity coordinates are employed and an interpolation is performed using the two closest *isotemperature* lines derived from a look-up table.

III. Experimental Issues

Several TIG (Tungsten Inert Gas) arc-welding tests with the welding setup described in [18] were performed to evaluate the performance of the proposed colorimetric analysis in terms of welding diagnostics. AISI-304 stainless steel plates were chosen for these experiments, with Argon used as protection gas.

Regarding the optical setup, two different spectrometers were mainly involved in the acquisition of the plasma optical spectra: an *Ocean Optics* STS (spectral range: 350-800nm, optical resolution: 1.2nm) and the *BWTek* Econic (spectral range: 197-968nm, optical resolution: 0.3nm). An *Ocean Optics* USB2000 was also considered, but its spectral range from 193 to 533 nm made it unsuitable for the colorimetric studies. Two optical fibers of core diameters 600 and 200 µm were also used to collect the plasma radiation during the welding process. It is worth noting that the colorimetric analysis requires a calibration of the spectrometer response (amplitude). This was performed using a calibration lamp (*Ocean Optics* DH-2000-CAL) with a known irradiance spectrum. Fig. 1 depicts the spectra measured for the two spectrometers considered in this study.

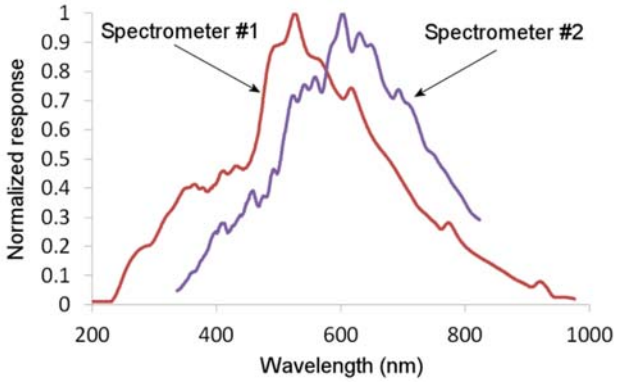

Fig. 1. Measured spectral responses of both spectrometers employed during the experimental tests.

One of the key points in this study lies in the analysis of the response of the spectroscopic and colorimetric monitoring parameters to different welding perturbations like variations in the welding current, protection gas flow rate, cut-off distance and so on. Fig. 2 (a) depicts a welding seam (bead-on-plate), where two perturbations have been provoked: a variation in the cut-off distance (separation between the tip of the electrode and the plate surface) of 1 mm and a shortage in the protection gas (Ar) flow. Both T_e profiles derived from the employment of the Boltzmann plot and the simplified methods (Eq. (1) and (2)) with Ar I lines have been depicted in Fig. 2 (b). The former (black dashed line) and the latter (red line) clearly indicate the perturbation associated with the variation of the cut-off distance performed between t ≈ 2.5 and t ≈ 3 s. However, these profiles do not allow to detect the perturbation associated with the protection gas flow cut, performed at t ≈ 7.5 s. The Ar I emission lines involved in the estimation of T_e are listed in Table II. The value of the coefficient of determination R^2 for the regression involved in the Boltzmann-plot method employed in the calculation of the T_e profile depicted in Fig. 2 is 0.99.

TABLE II
Chosen Ar I Emission Lines for T_E Estimation

λ (nm)	E_m (eV)	$\ln(I_{mn}\lambda_{mn}/A_{mn}g_{mn})$
675.2834	14.7425	7.0551
687.1289	14.7109	7.0717
696.5431	13.3278	8.6535
706.7218	13.3022	8.6708
727.2936	13.3279	8.6189
738.398	13.3022	8.6664
794.8176	13.2826	8.6620

The green thick line on Fig. 2 (b) depicts the color temperature profile that in this case shows a dip associated with the first perturbation, but also a clear indication of the gas flow cut with significant variations in terms of the temperature mean value.

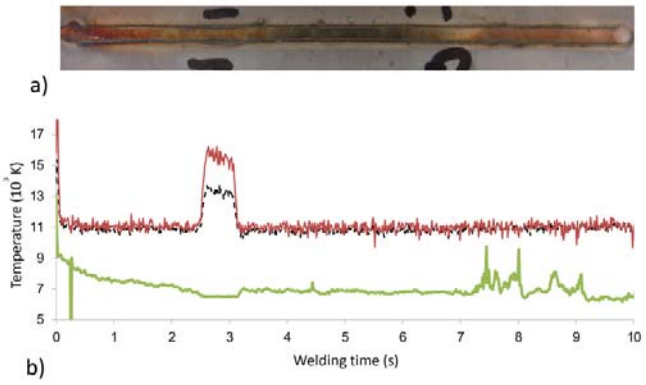

Fig. 2. Welding test with variation in the cut-off distance and protection gas shortage: (a) welding seam; and (b) electronic temperature profiles using Boltzmann-plot (black-dashed line), two ArI lines (red line) and the color temperature (green thick line).

This article has been accepted for publication in a future issue of this journal, but has not been fully edited. Content may change prior to final publication. Citation information: DOI 10.1109/JSEN.2015.2413057, IEEE Sensors Journal

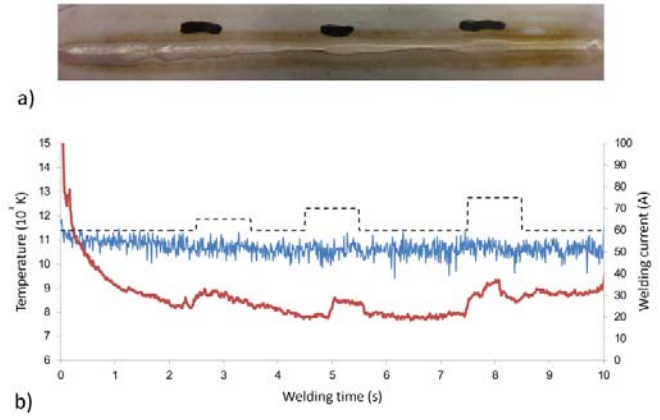

Fig. 3. (a) Welding seam with three variations in the welding current; (b) electronic temperature profile using Boltzmann-plot (blue line) versus the color temperature (red thick line) and the welding current (black-dashed line; right vertical axis).

The seam shown in Fig. 3 was performed with constant input parameters with the exception of the welding current. Its nominal value was established on 60 A, but changes to 65 (from t = 25 to t =35 s), 70 (from t = 45 to t =55 s) and 75 A (from t = 75 to t =85 s) were performed during the test. The T_e profile, calculated via the Boltzmann-plot method (blue line), does not show any clear perturbation correlated to the welding current changes. However, these three changes can be detected on the color temperature profile that also exhibits a decaying slope at the beginning of the process, probably due to the inherent instability associated with the start of the arc-welding process. To complete the colorimetric analysis of the welding test already presented in Fig. 3, the three parameters of the HSL color space have been also calculated and depicted in Fig. 4. While the luminance (green line) exhibits a profile with a rather low sensitivity to the process perturbations, both hue (blue line) and saturation (black line) allow a detection of the three events, especially the two final current changes. It is worth noting that the saturation profile is almost identical to the associated color temperature, and that the hue profile shows an inverse response to the mentioned events.

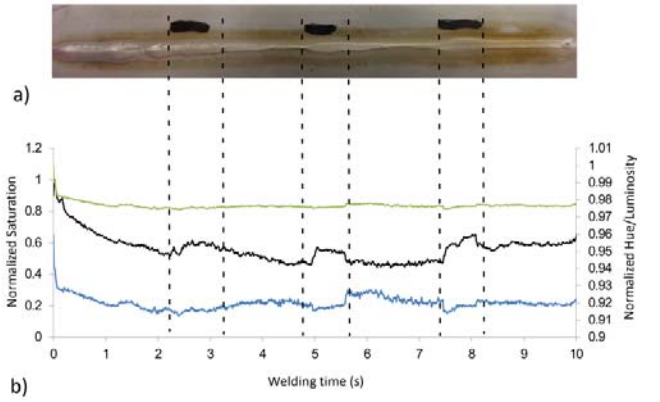

Fig. 4. (a) Welding seam with three variations in the welding current; (b) associated colorimetric analysis: profiles of hue (blue), saturation (black) and luminance (green line).

While the previous discussed results are derived from the employment of a specific spectrometer (*Econic BWTek*), a comparison on the performance of the two spectrometers already detailed at the beginning of this section has also been performed (spectrometer #1 (*BWTek* Econic) and #2 (*Ocean Optics* STS)). It is worth noting that these spectrometers have been chosen for this analysis given their different features in terms of spectral range, spectral response and optical resolution. In this case a bead-on-plate seam has been performed with three perturbations: a variation of the cut-off distance at x ≈ 2s, and two protection gas shortages at x ≈ 5.3 and x ≈ 8s (Fig. 5(a)). Both the plasma electronic temperature and the color temperature have been calculated with the data acquired with both devices and their profiles are presented in Fig. 5 (b) and (c). The effects provoked by the perturbations can be appreciated in Fig. 5(a), especially for the final gas shortage at x ≈ 8s.

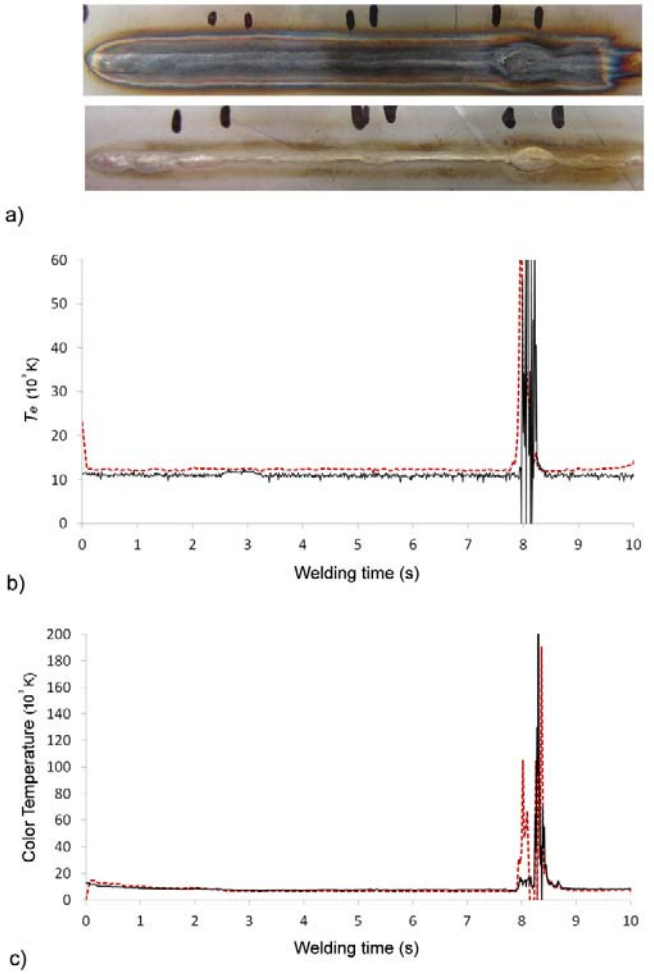

Fig. 5. (a) Welding seam with three perturbations (cut-off distance and two protection gas cuts); (b) profiles of the plasma electronic temperature for spectrometers #1 and #2; (c) profiles of the color temperature for spectrometers #1 and #2.

This article has been accepted for publication in a future issue of this journal, but has not been fully edited. Content may change prior to final publication. Citation information: DOI 10.1109/JSEN.2015.2413057, IEEE Sensors Journal

For both spectrometers and profiles the perturbation at x ≈ 8s gives rise to a significant variation in the output signals (T_e in blue and color temperature in red dashed line). However, the first two perturbations are not so clearly identified, although some subtle variations can be observed if a zoom is performed.

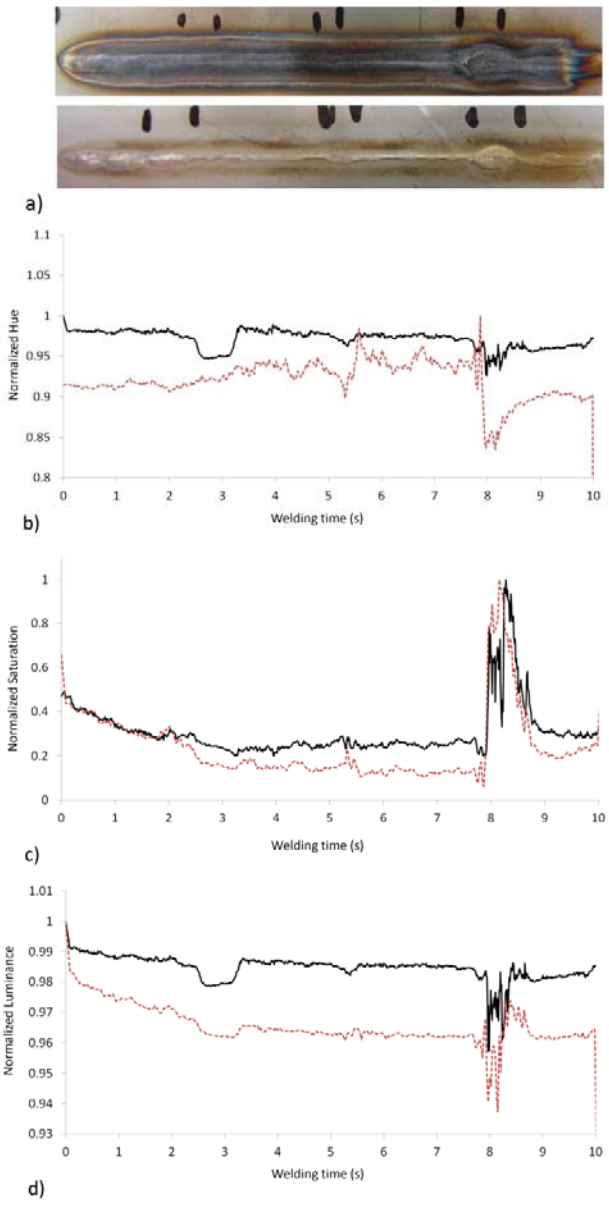

Fig. 6. (a) Welding seam with three perturbations (cut-off distance and two protection gas cuts); (b) profiles of the normalized hue for spectrometers #1 (black line) and #2 (red dashed line); (c) profiles of the normalized saturation for spectrometers #1 (black line) and #2 (red dashed line); (d) profiles of the normalized luminance for spectrometers #1 (black line) and #2 (red dashed line).

Fig. 6 depicts the obtained HSL parameters for spectrometer #1 (black line) and #2 (red dashed line). The analysis of these profiles allows to identify these possible weld flaws, especially the cut-off distance variation in Fig. 6(b) and (d) (hue and luminance, respectively), the first gas shortage in Fig. 6(b) (hue) and the second gas cut using the three parameters. In terms of quality monitoring, the luminance exhibits a good profile, less noisy and with a clear detection of the three events for both spectrometers. One of the reasons to explain the differences between the profiles obtained for both devices can be found in their different amplitude response, used to correct the acquired plasma spectra, and in the different spectral ranges considered.

To facilitate a more quantitative analysis on the ability of the different chosen parameters to allow a detection of the provoked perturbations, the defect sensitivity parameter S/N^* has been employed [9]. This parameter is calculated by estimating the signal-to-noise ratio over a segment of the profile where no perturbations have been generated; in this case the section between x = 6 and x = 7s has been chosen. Afterwards, the difference between the values of a given parameter (for example the color temperature) at a specific perturbation and a close region where the seam is supposed to be correct is obtained. Finally, the defect sensitivity is calculated by multiplying these two values. The study performed in this regard for the seam analyzed in Fig. (5) and (6) has been detailed in Table III, where both T_e and the color temperature data have been normalized.

TABLE III
DEFECT SENSITIVITY ANALYSIS

DEFECT SENSITIVITY

	Spectrometer #1			Spectrometer #2		
	P #1	P #2	P #3	P #1	P#2	P#3
T_e	0.591	0.091	25.689	0.938	0.341	100.949
Color Temp	0.007	0.040	6.421	0.088	0.290	15.095
Hue	20.173	7.401	20.865	2.022	6.764	14.756
Saturation	18.133	0.253	17.548	0.129	0.938	7.324
Luminance	21.769	8.622	72.675	13.378	3.587	86.138

It can be observed how this analysis shows that the best detection of the three perturbations is obtained using the hue and luminance parameters, especially for spectrometer #1.

The effect of the spectral responses of the chosen spectrometers and their considered calibrations can be appreciated in Fig. 7, where some of the results presented in Fig. 6 for spectrometer #2 have been compared with those obtained when the measured spectral response has not been taken into account in the process. It can be clearly observed how the profiles are somewhat different, for example exhibiting perturbations with opposite trends for both saturation and luminance. Although this might not affect the performance of the system in terms of defect detection, it can be appreciated how the defect sensitivity will change. In addition, this should be also considered if artificial intelligence solutions such as fuzzy logic or artificial neural networks are going to be involved in the monitoring systems.

This article has been accepted for publication in a future issue of this journal, but has not been fully edited. Content may change prior to final publication. Citation information: DOI 10.1109/JSEN.2015.2413057, IEEE Sensors Journal

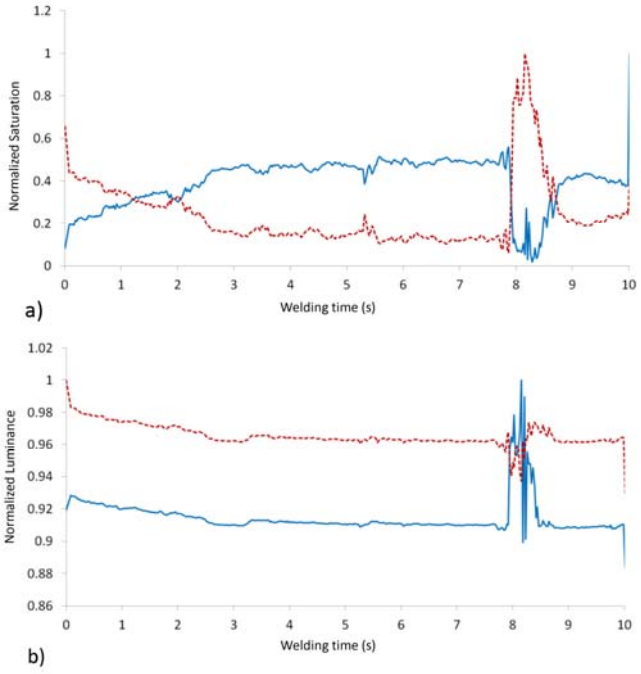

Fig. 7. (a) profiles of the normalized saturation for spectrometer #2 with (red dashed line) and without (blue solid line) considering its spectral response; (b) profiles of the normalized luminance for spectrometer #2 with (red dashed line) and without (blue solid line) considering its spectral response.

IV. Conclusions

A detailed analysis on the feasibility of using a colorimetric approach for online welding diagnostics has been discussed in this paper. Four different parameters, the color temperature and the hue, saturation and luminance derived from the HSL color space have been considered for monitoring purposes. The studies have shown how this approach exhibits better results in terms of defect detection in some particular scenarios in comparison to the traditional plasma electronic temperature profiles.

In particular, the color temperature and the HSL parameters have given rise to a better performance for the detection of changes in the welding current and protection gas shortages. A quantitative study on the defect detection ability of the chosen variables has been performed by using the so called defect sensitivity parameter. It is worth noting that this approach allows to avoid the emission line identification stage, thus enabling a more efficient solution in terms of computational performance, but also giving rise to the possibility of designing significantly less expensive monitoring systems. In this regard it would be highly interesting to explore the performance of tricolor photodiodes.

Further experiments with an extended defectology and in various welding frameworks are currently being considered to thoroughly understand the different behaviors of the monitoring parameters under analysis.

Acknowledgment

This work has been supported by the project TEC2013-47264-C2-1-R.

References

[1] G.-j. Zhang, Z.-h. Yan, and L. Wu, “Visual sensing of weld pool in variable polarity TIG welding of aluminium alloy,” Transactions of nonferrous metals society of china, vol. 16, no. 3, pp. 522-526, 2006.

[2] B. Abdullah, J. Smith, W. Lucas, J. Lucas, and F. Malek, "Monitoring of TIG welding using laser and diode illumination sources: a comparison study," in Electronic Design, 2008. ICED 2008. International Conference on, 2008, pp. 1-4.

[3] U. Sreedhar, C. Krishnamurthy, K. Balasubramaniam, V. Raghupathy, and S. Ravisankar, "Automatic defect identification using thermal image analysis for online weld quality monitoring," Journal of Materials Processing Technology, vol. 212, pp. 1557-1566, 2012.

[4] A. Tarn and D. Hardt, "Weld pool impedance for pool geometry measurement: stationary and non-stationary pools," Journal of dynamic systems, measurement, and control, vol. 111, p. 545, 1989.

[5] H. Gu and W. Duley, "A statistical approach to acoustic monitoring of laser welding," Journal of Physics D: Applied Physics, vol. 29, p. 556, 1996.

[6] A. Ancona, V. Spagnolo, P. M. Lugara, and M. Ferrara, "Optical Sensor for real-time Monitoring of CO2 Laser Welding Process," Applied Optics, vol. 40, pp. 6019-6025, 2001.

[7] J. Mirapeix, A. Cobo, C. Jaúregui, and J. López-Higuera, "Fast algorithm for spectral processing with application to on-line welding quality assurance," Measurement Science and Technology, vol. 17, p. 2623, 2006.

[8] J. Mirapeix, A. Cobo, S. Fernandez, R. Cardoso, and J. Lopez-Higuera, "Spectroscopic analysis of the plasma continuum radiation for on-line arc-welding defect detection," Journal of Physics D: Applied Physics, vol. 41, p. 135202, 2008.

[9] P. B. Garcia-Allende, J. Mirapeix, O. M. Conde, A. Cobo, and J. M. Lopez-Higuera, "Defect detection in arc-welding processes by means of the line-to-continuum method and feature selection," Sensors, vol. 9, pp. 7753-7770, 2009.

[10] J. Mirapeix, A. Cobo, J. Fuentes, M. Davila, J. M. Etayo, and J.-M. Lopez-Higuera, "Use of the plasma spectrum rms signal for arc-welding diagnostics," Sensors, vol. 9, pp. 5263-5276, 2009.

[11] F. Zhiwei, Z. Pu, and L. Wenzhong, "Application of Measurement Based on Three Primary-color Method in Welding Temperature Field [J]," Computer Automated Measurement & Control, vol. 3, 2005.

[12] D. A. Kerr, "The CIE XYZ and xyY Color Spaces," ed: Issue, 2010.

[13] G. Wyszecki and W. S. Stiles, Color science vol. 8: Wiley New York, 1982.

[14] Y. Ohno, "CIE fundamentals for color measurements," in NIP & Digital Fabrication Conference, 2000, pp. 540-545.

[15] H. S. Fairman, M. H. Brill, and H. Hemmendinger, "How the CIE 1931 color-matching functions were derived from Wright-Guild data," Color Research & Application, vol. 22, pp. 11-23, 1997.

[16] A. Ford and A. Roberts, "Colour space conversions," Westminster University, London, vol. 1998, pp. 1-31, 1998.

[17] A. R. Robertson, "Computation of correlated color temperature and distribution temperature," JOSA, vol. 58, pp. 1528-1535, 1968.

[18] L. Rodriguez-Cobo, R. Ruiz-Lombera, O. M. Conde, J.-M. López-Higuera, A. Cobo, and J. Mirapeix, "Feasibility study of Hierarchical Temporal Memories applied to welding diagnostics," Sensors and Actuators A: Physical, vol. 204, pp. 58-66, 2013.